

# CORRELATIONS BETWEEN THERMOELECTRIC PROPERTIES AND LATTICE COMPRESSION IN Al-ZnO CERAMICS

Wiff J.P., Kinemuchi Y., Kaga H., Ito C. and Watari K.

National Institute of Advanced Industrial Science and Technology (AIST), Nagoya 463-8560, Japan

Contact author: y.kinemuchi@aist.go.jp

## Abstract

This work studies the influence of additive amount on the lattice distortion, effective mass and thermoelectric properties of doped-ZnO ceramics. The results indicate that as the ion additive amount increases the ZnO lattice is compressed and the effective mass increases, thus enhancing the thermoelectric behavior in the doped-ZnO ceramics.

## Introduction

Doped ZnO has been widely studied for optical applications; moreover it has been evaluated for thermoelectrical applications due to its chemical stability at high temperatures<sup>1</sup>, recently Alahmed *et al.* used first-principle density functional calculations for studying the effect of biaxial loadings on the ZnO lattice, band structure and effective mass<sup>2</sup>. They showed that as increasing the tensile strain along ab plane on the ZnO lattice, the  $c/a$  lattice ratio decreases and the effective mass ( $m^*$ ) rises slightly.

This work focuses on an experimental evidence of predictions by Alahmed *et al.* in the case of ZnO lattice distortions caused by ion doping (for example  $Al^{+3}$ ) and its influence on the lattice structure, effective mass and subsequent thermoelectric properties.

## Experimental procedure

$Zn_{1-x}Al_xO$  samples with  $x=\{0.001, 0.005, 0.01, 0.02, 0.03 \text{ or } 0.05\}$  were prepared by solid-state reaction of ZnO and  $\gamma-Al_2O_3$  powders.

Powders, in stoichiometric quantities, were mixed and milled in a polyethylene bottle, containing ethanol and ZrO balls, at

100 rpm for 20 h. Afterwards powders were dried and hydrostatically cold-pressed under 100 MPa for 1 min. Finally, pellets were sintered in air at 1400°C for 8 h at a heating rate of 10°C/min. After sintering, all samples exhibited densities over 99% with respect to the theoretical compositions.

X-ray diffraction (XRD) in  $\theta$ - $2\theta$  configuration with  $CuK_\alpha$  radiation at 40 kV and 200 mA was used for determining the lattice constants by least-squares method. The thermoelectric characterization (Seebeck coefficient ( $\alpha$ ) and electrical resistivity ( $\rho$ )) was performed simultaneously via ULVAC-ZEM1 equipment from room temperature (RT) to 800°C. Carrier concentration ( $n$ ) and Hall mobility ( $\mu$ ) were determined by using Hall measurement at RT.

## Results and discussions

Fig. 1 shows the XRD patterns of  $Zn_{1-x}Al_xO$   $x=\{0.001, 0.005, 0.01, 0.02, 0.03 \text{ or } 0.05\}$  samples. All samples contain ZnO as main phase, however spinel  $ZnAl_2O_4$  also was detected as secondary phase, being dominant at  $x > 0.01$  (1 at%).

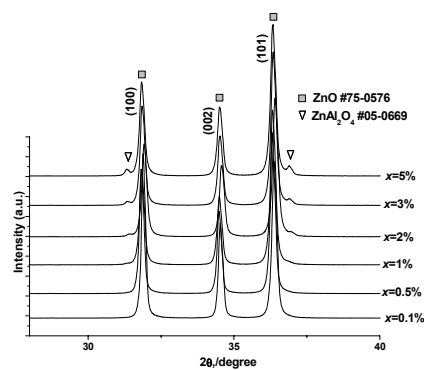


Fig. 1 XRD patterns of  $Zn_{1-x}Al_xO$  samples

In general, the lattice parameter  $a$  tends to increase and  $c$  to decrease as the additive concentration rises (not shown). Fig. 2 shows the  $c/a$  lattice ratio for all samples. It is clear that as the Al additive amount increases the ZnO lattice is compressed along  $c$ -axis up to the limit value of  $c/a = 1.6010$

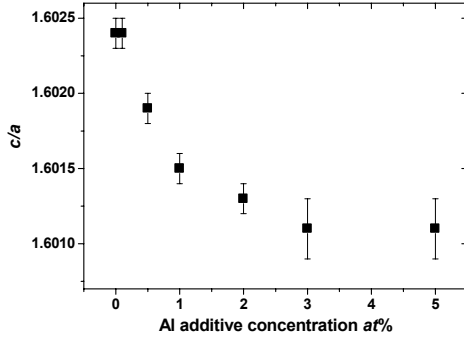


Fig. 2  $c/a$  lattice ratio as a function of Al additive concentration

It is reasonable to assume that as the additive concentration increases the strain in the ZnO lattice also increases because the ionic radius of Al is smaller than that of Zn. This is similar to the tendency predicted by Alahmed et al using first-principle density functional calculations<sup>2</sup>. In that work, the authors found proportionality between the  $c/a$  and in plane tensile strain.

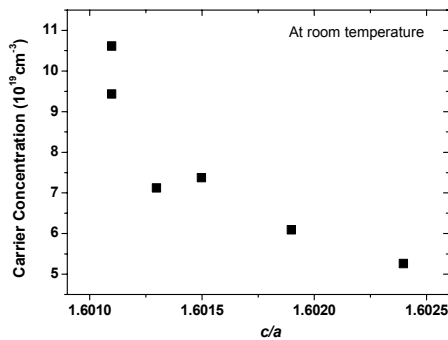


Fig. 3 Carrier concentration as a function of  $c/a$  lattice ratio

Fig. 3 shows the carrier concentration as a function of  $c/a$  lattice ratio, indicating a non-linear behavior. As the ZnO lattice is compressed from  $c/a=1.6024$  up to  $c/a=1.6014$ , the carrier concentration slightly increases; however, at higher compressions of  $c/a$  ratio the carrier

concentration rises up to a limit value around  $1 \times 10^{20} \text{ cm}^{-3}$ .

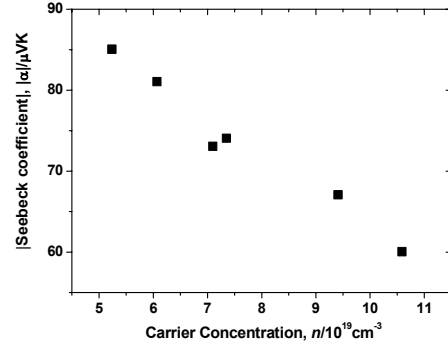


Fig. 4 Absolute value of Seebeck coefficient as a function of carrier concentration

Fig. 4 shows the absolute value of Seebeck coefficient ( $\alpha$ ) as a function of carrier concentration. Seebeck coefficient increases as the carrier concentration decreases, which agrees with the model proposed by Jonker<sup>3</sup>.

$$\alpha = -\frac{k_B}{e} \left( \ln \left( \frac{N_c}{n} \right) + A \right) \quad (1)$$

Where  $k_B$  is the Boltzmann constant,  $e$  is electron charge and  $A$  corresponds to a transport term. Hereinafter and just for simplicity the  $A$  term will be considered constant.

In order to evaluate the effective mass, the following equations are used:

$$\alpha = -\frac{k_B}{e} \left( \frac{(r+2)F_{r+1}(\eta^*)}{(r+1)F_r(\eta^*)} - \eta^* \right) \quad (2)$$

where,  $\eta^* = \frac{\eta}{k_B T}$  is the reduced Fermi level, and  $F_r$  is the Fermi integral of order  $r$ .

$$F_r = \int_0^{\infty} \frac{x^r}{1 + \exp(x - \eta^*)} dx \quad (3)$$

The parameter  $r$  is called scattering parameter and it depends on the scattering mechanism at a given temperature. A reasonable value for  $r$  at room temperature can be assumed to be  $r=0.5^4$ .

Besides, in the general case, the carrier concentration can be expressed as following<sup>5</sup>:

$$n = 5.437 \times 10^{15} \left( \frac{m^*}{m_0} T \right)^{3/2} \int_0^\infty \frac{\varepsilon^{1/2} (1 + \beta\varepsilon)^{1/2} (1 + 2\beta\varepsilon)}{1 + \exp(\varepsilon - \eta^*)} d\varepsilon \quad (4)$$

Where  $h$  is the Planck's constant and  $\beta$  gives the degree of deviation of the conduction band from parabolicity. Thus, assuming  $\beta=0.1$  the effective mass can be estimated by resolving numerically the previous equations at RT. The effective mass just slightly increases from 0.27 to  $0.30m_0$  as the lattice is compressed.

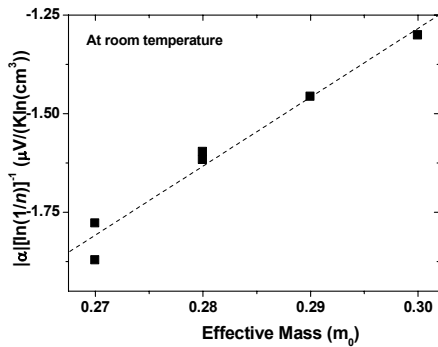


Fig. 5 Net contribution of effective mass to Seebeck coefficient

Fig. 5 shows the absolute value of Seebeck coefficient at RT as a function of effective mass. Here, Seebeck coefficient is normalized by  $\ln(1/n)$  in order to cancel the carrier concentration contribution (see equation 1). Fig. 5 shows that as increasing the effective mass an enhancement on the net Seebeck coefficient is induced.

Unfortunately, the variation of effective mass is quite small, so it is hard to distinguish the contributions of lattice compression to the variation of effective mass from non-parabolicity of ZnO band structure. However, the effective mass enhancement as a function of  $c/a$  lattice compression has been predicted by first-principle calculations<sup>2</sup>, suggesting that the  $c/a$  ratio could play a role in the enhancement of the effective mass.

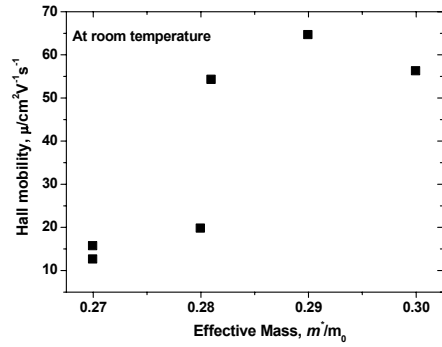


Fig. 6 Hall mobility as a function of effective mass

Fig. 6 shows Hall mobility as a function of the effective mass. Considering Drude's formulation, Hall mobility could be expressed in terms of electron charge ( $e$ ), carrier collision time ( $\tau$ ), and effective mass ( $m^*$ ) as follows:

$$\mu = \frac{e\tau}{m^*} \quad (5)$$

But, evidently, the tendency showed in Fig. 6 contradicts this equation. An explanation to this discrepancy in the Hall mobility behavior could be made considering a model proposed by Srikant *et al*<sup>6</sup>.

In this model, the defects are mainly located at grain boundaries acting as carrier traps. Thus, a potential barrier will be induced at the grain boundary. The magnitude of this barrier depend on carrier concentration; this is due to that a significant proportion of total carriers will be trapped at the grain boundary at a low carrier concentration, reducing the apparent mobility through the material, and contrarily, the proportion of total carriers trapped at the grain boundary decreases at a high carrier concentration and therefore the apparent mobility should increase. Thus, Hall mobility is mainly affected by the carrier traps at grain boundaries not by the change in effective mass or  $c/a$  lattice ratio.

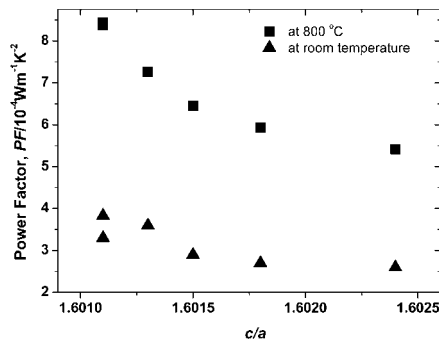


Fig. 7 Power factor as a function of  $c/a$  lattice ratio

Fig. 7 shows power factor as a function of  $c/a$  ratio measured at RT and 800°C. The highest power factor is achieved at the highest  $c/a$  compressions,  $3.9$  and  $8.5 \times 10^{-4} \text{ Wm}^{-1} \text{ K}^{-2}$  at RT and 800°C, respectively. A change in the slope is observed around  $c/a = 1.6014$ , suggesting that a high carrier concentration is required to enhance the power factor.

### Conclusion

Sintered  $\text{Zn}_{1-x}\text{Al}_x\text{O}$  samples were thermoelectrically characterized from room temperature up to 800°C. The lattice ratio  $c/a$  was used for proposing an explanation of doping effect on the Seebeck coefficient, effective mass, and power factor. As the doped ZnO lattice is compressed (low  $c/a$  ratio), the slight increase of effective mass enhances its net contribution to the Seebeck coefficient.

Additionally, the results suggested that maximum carrier concentration should be limited by high  $c/a$  compressions due to geometrical restrictions, whereas the Hall mobility is mainly affected by a change of microstructure or defects. It was also found that as the  $c/a$  a correlation with the maximum power factor in this kind of ceramics ( $8.5 \times 10^{-4} \text{ Wm}^{-1} \text{ K}^{-2}$  at 800°C). Finally, in ion-doped ZnO system a high compression lattice, due to heavy doping, could be a key for improving the power factor.

### References

1. Ohtaki *et al.* J. Appl. Phys. 79(3) (1996) 1816-1818.
2. Alahmed *et al.* Phys. Rev. B 77 (2008) 045213.
3. Jonker G. Phillips Res. Rep. 23 (1968) 131-138.
4. Young *et al.* J. Vac. Sci. Technol. A 18(6) (2000) 2978-2985.
5. Bhan *et al.* Semicond. Sci. Technol. 19(3) (2004) 413-416.
6. Srikant *et al.* J. Am. Ceramics Soc. 78(77) (1995) 1935-39.